Optically pumped intersubband emission of short-wave infrared radiation with GaN/AlN quantum wells

Kristina Driscoll, Yitao Liao, Anirban Bhattacharyya, Lin Zhou, David J. Smith, Theodore D. Moustakas, and Roberto Paiella

Citation: Applied Physics Letters **94**, 081120 (2009); doi: 10.1063/1.3089840
View online: http://dx.doi.org/10.1063/1.3089840
View Table of Contents: http://scitation.aip.org/content/aip/journal/apl/94/8?ver=pdfcov
Published by the AIP Publishing

Optically pumped intersubband emission of short-wave infrared radiation with GaN/AlN quantum wells

Kristina Driscoll,[1] Yitao Liao,[1] Anirban Bhattacharyya,[1] Lin Zhou,[2] David J. Smith,[2] Theodore D. Moustakas,[1] and Roberto Paiella[1,a)]
[1]*Department of Electrical and Computer Engineering and Photonics Center, Boston University, 8 Saint Mary's Street, Boston, Massachusetts 02215, USA*
[2]*Department of Physics, Arizona State University, Tempe, Arizona 85287, USA*

(Received 26 December 2008; accepted 8 February 2009; published online 27 February 2009)

Optically pumped pulsed emission of short-wave infrared radiation based on intersubband transitions in GaN/AlN quantum wells is demonstrated. Nanosecond-scale pump pulses are used to resonantly excite electrons from the ground states to the second-excited subbands, followed by radiative relaxation into the first-excited subbands. The measured room-temperature output spectra are peaked near 2 μm with integrated powers of a few hundred nanowatts. The intersubband origin of the measured luminescence is confirmed via an extensive study of its polarization properties and pump wavelength dependence, as well as simulations of the quantum well subband structure. © *2009 American Institute of Physics*. [DOI: 10.1063/1.3089840]

Intersubband (ISB) transitions in semiconductor quantum wells (QWs) exhibit several desirable features for many optoelectronic device applications. So far, they have been primarily explored in As-based III-V materials, whose relatively small conduction-band offsets ΔE_c limit the operating wavelengths to values >3 μm, i.e., in the midwave infrared range and beyond. Recently, however, novel materials systems with larger conduction-band offsets have also been considered for the purpose of extending the operation of ISB devices to shorter wavelengths. Particularly promising in this respect are GaN/Al(Ga)N QWs where ΔE_c can be as large as 1.75 eV. Consequently, these heterostructures can accommodate ISB transitions at wavelengths throughout the short-wave infrared spectral region, including the low-loss transmission window of silica optical fibers.

In recent years, ISB absorption in isolated and coupled GaN/Al(Ga)N QW structures has been extensively studied by several groups.[1–6] A number of ISB device functionalities based on these heterostructures have also been demonstrated, including photodetection,[7,8] electro-optic modulation,[9] and ultrafast all-optical switching.[10,11] Regarding light emission, various nitride-based electrically and optically pumped ISB laser structures have been proposed and theoretically investigated.[12–14] On the experimental side, however, the progress so far has been limited to one report of cw photoluminescence in the 2.13–2.3 μm range with exceedingly small output powers ($\sim$10 pW) requiring highly sensitive lock-in detection techniques.[15] In this letter, we describe the measurement of ISB light emission from GaN/AlN QWs pumped with a pulsed optical parametric oscillator (OPO), yielding peak output powers of a few hundred nanowatts. The output spectra are peaked at wavelengths near 2.05 μm, which represent a new record for the shortest ISB emission wavelength from any QW materials system.

The material used in this work was grown on a (0001) sapphire substrate by rf plasma-assisted molecular beam epitaxy. Following nitridation of the substrate, a 1-μm-thick AlN buffer layer was deposited to serve as a template for growth of the subsequent GaN/AlN layers. The sample active region consists of 200 periods of nominally 18-Å-thick GaN wells (doped *n*-type to the level of $\sim 2\times10^{19}$ cm^{-3}) separated by 26-Å-thick AlN barriers. During deposition of the AlN layers a small Ga flux was used as a surfactant to promote two-dimensional growth. Finally, the multiple-QW structure was terminated with a 70-nm-thick AlN capping layer. The sample microstructure was studied using a 400 keV JEM-4000EX transmission electron microscope (TEM). As illustrated in Fig. 1(a), cross-sectional TEM images reveal high structural quality with smooth interfaces and good control of the structure periodicity. Some period-to-period and in-plane thickness variations are visible, but they are limited to about 1 ML, with the GaN well and AlN barrier thicknesses estimated to be in the range of 6–8 and 9–10 ML (with 1 ML$\approx$2.6 Å), respectively.

The QW ISB absorption properties were studied at room temperature using a Fourier transform infrared (FTIR) spectrometer and a liquid-nitrogen-cooled HgCdTe detector. For

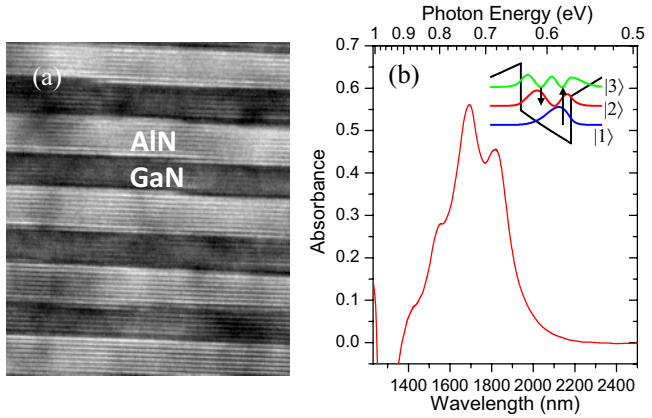

FIG. 1. (Color online) (a) Cross-sectional TEM image of the QW sample used in this work. (b) Room-temperature ISB absorbance spectrum of the same sample. The negative dip in the spectrum near 1300 nm is an artifact of the system response and is not related to the optical properties of the sample. The inset shows the calculated conduction-band lineup and squared envelope functions of the three lowest bound states (referenced to their respective energy levels) of one QW in the active region.

a)Electronic mail: rpaiella@bu.edu.

this measurement, the substrate side of the sample was mirror polished and two opposite facets were lapped at 45° to obtain a multipass waveguide geometry. Light from the FTIR internal source was coupled in and out at normal incidence through these facets. Due to the polarization selection rules of ISB transitions, only TM-polarized light is absorbed in the QWs. A measured absorbance spectrum normalized with respect to the system response is plotted in Fig. 1(b), where the observed feature is ascribed to ISB transitions between the ground states $|1\rangle$ and the first-excited subbands $|2\rangle$. It should be noted that the $|1\rangle \rightarrow |3\rangle$ transitions are also allowed in these QWs, due to the built-in electric fields of nitride heterostructures, which partially break the symmetry of the bound-state envelope functions. However, the resulting absorption is still too weak to be unambiguously resolved in our FTIR transmission spectra.

The multipeaked nature of the absorbance spectrum of Fig. 1(b) is attributed to the monolayer-scale variations in the QW thicknesses, which give rise to fluctuations in the ISB transition energies.[4] To confirm this interpretation, the GaN/AlN QWs were modeled using a self-consistent Poisson and Schrödinger equations solver, which includes the characteristic pyro- and piezoelectric fields of nitride heterostructures and the conduction-band nonparabolicity. All the relevant material parameters were taken from Ref. 16. Using this model, the three peaks observed in the measured absorbance spectrum can be attributed to $|1\rangle \rightarrow |2\rangle$ ISB transitions in 6-, 7-, and 8-ML-thick QWs, with all calculated energies within less than 7% of the experimental values. The inset of Fig. 1(b) depicts the calculated conduction-band lineup and bound-state squared envelope functions of a 18-Å-thick (7 ML) QW. The calculated energies of the $|1\rangle \rightarrow |2\rangle$ and $|2\rangle \rightarrow |3\rangle$ ISB transitions in this case are 699 and 633 meV, respectively.

For the light emission measurements, a pulsed OPO was used to optically pump electrons from $|1\rangle$ to $|3\rangle$, followed by relaxation into $|2\rangle$ and corresponding luminescence at the $|3\rangle \rightarrow |2\rangle$ transition energy. The OPO output consists of a train of pulses with 5 ns width and 20 Hz repetition rate. Its average power, as measured with a pyroelectric detector, is approximately 10 mW, corresponding to a pulse peak power of 100 kW. The measurements were carried out at room temperature, with the sample input and output facets polished at 45° and 90°, respectively. The pump light was delivered to the sample with a multimode optical fiber, and then focused at normal incidence onto the 45° input facet with a two-lens imaging system, producing an estimated spot diameter of about 300 μm. Broadband quarter- and half-wave retarders placed before the fiber and a polarizer before the sample were used to recover and subsequently filter the desired state of linear polarization for the pump light exiting the fiber. The emitted light was collected from the 90° output facet and focused onto the entrance slit of a monochromator by a second two-lens imaging system (with an F/1 collection lens and a germanium plate in place to reject any residual pump light). The monochromator output light was finally measured using a room-temperature extended-range InGaAs detector with 1.2–2.6 μm spectral response and 45 MHz bandwidth. To increase the measurement sensitivity, gated detection was performed using a box-car integrator.

Figure 2 shows two spectra measured at different positions of the QW sample using a TM-polarized pump at λ_p =910 nm (1.362 eV). The solid lines in the figure are fits to

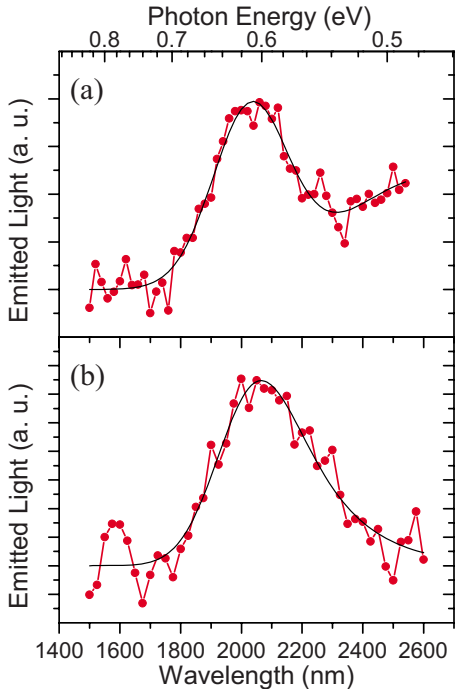

FIG. 2. (Color online) Emission spectra measured with a TM-polarized pump wave at 910 nm (dotted lines), and modified-Gaussian fits of the experimental data (solid lines). The spectra in (a) and (b) were measured at two different places in the QW sample.

a modified Gaussian peak, superimposed on a broad pedestal in the case of Fig. 2(a). The photon energies of peak emission and the spectral full widths at half maximum obtained from these fits are 608 meV (2.04 μm) and 99 meV in Fig. 2(a), and 602 meV (2.06 μm) and 105 meV in Fig. 2(b). These two spectra illustrate the reproducibility of well-resolved luminescence features across the sample area. The experimental photon energies of peak emission are close to the calculated value of the $|3\rangle \rightarrow |2\rangle$ transition energy [633 meV in 7-ML-thick QWs, as in the inset of Fig. 1(b)]. Furthermore, they are in good agreement (well within the emission linewidth) with the difference between the pump photon energy used in the measurements and the experimental value of 735 meV for the $|1\rangle \rightarrow |2\rangle$ transition energy estimated from Fig. 1(b). These observations provide strong evidence that the observed emission is indeed due to optical pumping from $|1\rangle$ to $|3\rangle$ followed by radiative relaxation from $|3\rangle$ to $|2\rangle$. Incidentally, a comparison between Fig. 2 and Fig. 1(b) also suggests that the $|2\rangle \rightarrow |1\rangle$ transitions do not give any appreciable contribution to the detected light.

Further experimental evidence of the ISB nature of the measured luminescence is summarized in Fig. 3. Figure 3(a) shows two spectra measured at the same spot under identical conditions except for the pump polarization, which is rotated from TM to TE. Essentially no emission is detected in the latter case, consistent with the polarization selection rules of ISB transitions. In Fig. 3(b) we plot two spectra obtained using the same TM-polarized pump wave [at λ_p=910 nm as in Figs. 2 and 3(a)], and with a polarizer added to the collection optics after the sample. As expected for ISB light emission, the luminescence is largely TM-polarized, with a strong reduction (by a factor of over 3) in the integrated power when the polarizer transmission axis is rotated from TM to TE. The small fraction of detected TE light is attributed to polarization scrambling of the TM-polarized ISB

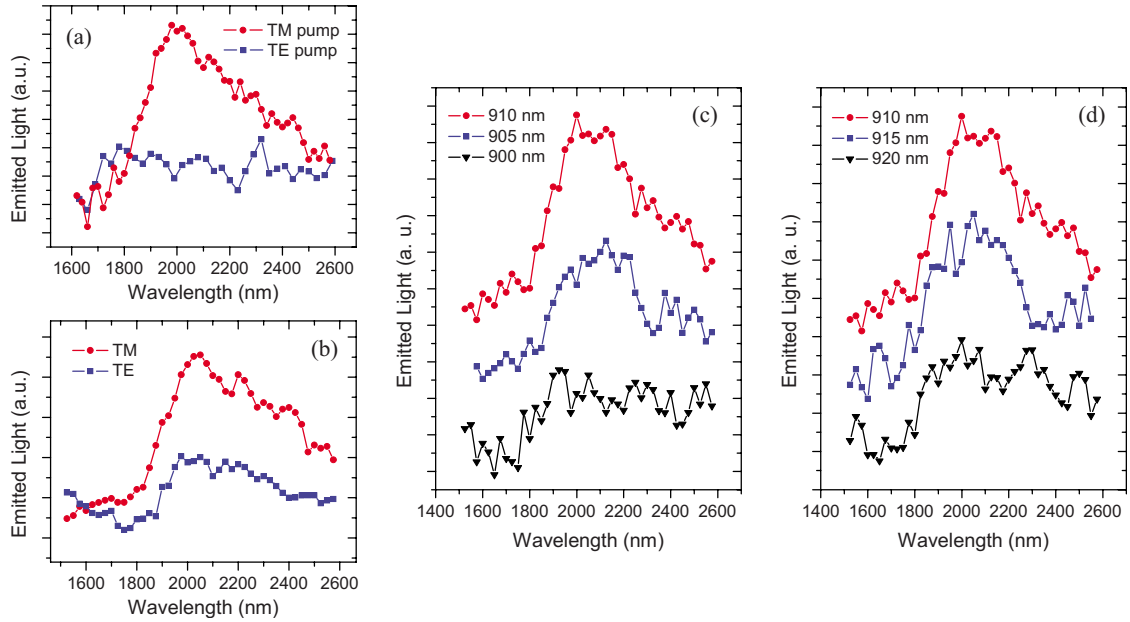

FIG. 3. (Color online) Emission spectra obtained under various excitation conditions. (a) Luminescence spectra measured with otherwise identical TM- (circles) and TE- (squares) polarized pump waves. (b) Luminescence spectra measured with the same pump wave and passed through a polarizer with transmission axis oriented along the TM (circles) and TE (squares) directions. (c) Dependence of the emission spectrum on the pump wavelength for $\lambda_p \leq 910$ nm. (c) Dependence of the emission spectrum on the pump wavelength for $\lambda_p \geq 910$ nm. In (c) and (d) the spectra are shifted relative to one another vertically for the sake of illustration clarity.

emission as it traverses the sample, due to the residual roughness in the bottom surface and sidewalls. Finally, Figs. 3(c) and 3(d) show the evolution of the luminescence spectrum versus pump wavelength λ_p for TM-polarized pump light. The emitted intensity is found to be highly dependent on λ_p and to be peaked around $\lambda_p = 910$ nm, close to the calculated value of the $|1\rangle \rightarrow |3\rangle$ transition wavelength [931 nm in Fig. 1(b)]. This resonant behavior is again consistent with optically pumped ISB light emission.

The peak integrated power of the detected light pulses is on the order of a few hundred nanowatts, with typical values of about 300 nW. Besides the low collection efficiency of the measurement setup, these values are mainly limited by the very inefficient $|1\rangle \rightarrow |3\rangle$ pump absorption, which is only weakly allowed in these uncoupled QWs by the parity-breaking action of the internal electric fields. As a result, only a negligible fraction of the incident pump power is actually absorbed in the sample. The estimated ISB radiative efficiency at room temperature (based on calculated dipole moments and nonradiative lifetimes) is 4×10^{-6}, which is on par with that of uncoupled QWs based on other materials systems. Compared to the only previous report of optically pumped ISB light emission with GaN/AlN QWs,[15] our measured power levels are over four orders of magnitude higher, mainly due to the proportionally higher peak pump power allowed by our pulsed excitation scheme. These results therefore show that, despite the complexities of nitride heterostructures, large electronic populations in excited subbands can be established, and the resulting ISB light emission scales linearly with the excitation level over an extensive range spanning several orders of magnitude. This is an important requirement for the demonstration of nitride-based short-wavelength ISB lasers. Future work in that direction will focus on the development of more advanced QW structures providing sufficiently large pumping efficiency and the possibility of robust population inversion.

This work was supported by the National Science Foundation under Grant No. ECS-0622102. We acknowledge use of facilities in the John M. Cowley Center for High Resolution Electron Microscopy at Arizona State University.

[1] C. Gmachl, H. M. Ng, S.-N. G. Chu, and A. Y. Cho, Appl. Phys. Lett. **77**, 3722 (2000).
[2] J. Hamazaki, S. Matsui, H. Kunugita, K. Ema, H. Kanazawa, T. Tachibana, A. Kikuchi, and K. Kishino, Appl. Phys. Lett. **84**, 1102 (2004).
[3] I. Friel, K. Driscoll, E. Kulenica, M. Dutta, R. Paiella, and T. D. Moustakas, J. Cryst. Growth **278**, 387 (2005).
[4] M. Tchernycheva, L. Nevou, L. Doyennette, F. H. Julien, E. Warde, F. Guillot, E. Monroy, E. Bellet-Amalric, T. Remmele, and M. Albrecht, Phys. Rev. B **73**, 125347 (2006).
[5] M. Tchernycheva, L. Nevou, L. Doyennette, F. H. Julien, F. Guillot, E. Monroy, T. Remmele, and M. Albrecht, Appl. Phys. Lett. **88**, 153113 (2006).
[6] K. Driscoll, A. Bhattacharyya, T. D. Moustakas, R. Paiella, L. Zhou, and D. J. Smith, Appl. Phys. Lett. **91**, 141104 (2007).
[7] D. Hofstetter, S.-S. Schad, H. Wu, W. J. Schaff, and L. F. Eastman, Appl. Phys. Lett. **83**, 572 (2003).
[8] A. Vardi, G. Bahir, F. Guillot, C. Bougerol, E. Monroy, S. E. Schacham, M. Tchernycheva, and F. H. Julien, Appl. Phys. Lett. **92**, 011112 (2008).
[9] L. Nevou, N. Kheirodin, M. Tchernycheva, L. Meignien, P. Crozat, A. Lupu, E. Warde, F. H. Julien, G. Pozzovivo, S. Golka, G. Strasser, F. Guillot, E. Monroy, T. Remmele, and M. Albrecht, Appl. Phys. Lett. **90**, 223511 (2007).
[10] N. Iizuka, K. Kaneko, and N. Suzuki, IEEE J. Quantum Electron. **42**, 765 (2006).
[11] Y. Li, A. Bhattacharyya, C. Thomidis, T. D. Moustakas, and R. Paiella, Opt. Express **15**, 5860 (2007).
[12] V. D. Jovanović, Z. Ikonić, D. Indjin, P. Harrison, V. Milanović, and R. A. Soref, J. Appl. Phys. **93**, 3194 (2003).
[13] V. D. Jovanović, D. Indjin, Z. Ikonić, and P. Harrison, Appl. Phys. Lett. **84**, 2995 (2004).
[14] E. Bellotti, K. Driscoll, T. D. Moustakas, and R. Paiella, Appl. Phys. Lett. **92**, 101112 (2008).
[15] L. Nevou, M. Tchernycheva, F. H. Julien, F. Guillot, and E. Monroy, Appl. Phys. Lett. **90**, 121106 (2007).
[16] I. Vurgaftman and J. R. Meyer, J. Appl. Phys. **94**, 3675 (2003).